8.3 APPLICATION OF A 3-D URBAN SURFACE-SENSOR-SUN MODEL TO ESTIMATE URBAN THERMAL ANISOTROPY FOR A RANGE OF URBAN GEOMETRIES

James A. Voogt
[1]University of Western Ontario, London ON CANADA

1. INTRODUCTION

Anisotropy (directional variation) of upwelling thermal radiation complicates remote sensing of urban surface temperatures. The anisotropy is created through the combination of a three-dimensionally rough urban surface, sensor viewing geometry and varying solar loading (daytime) or cooling (nighttime) that creates strong microscale contrasts of surface temperature that depend on facet orientation and type. Urban thermal anisotropy has been observed (e.g. Voogt and Oke 1998) and shown to be large with respect to the anisotropy of other natural or agricultural surfaces.

Direct observations of urban thermal anisotropy are expensive, typically necessitating aircraft based sensors to provide suitable spatial resolution and control over viewing direction. These costs generally preclude high temporal resolution assessments of multiple land uses or different cities. To expand our knowledge, the construction of numerical models that can represent the urban thermal anisotropy is needed. One such model is the SUM surface-sensor-sun relations model Soux et al. (2004). This model calculates how a remote sensor views a simple urban surface by calculating the *radiative source area* or view factors of the urban surface components for a given remote sensor position. When combined with surface temperature information, it is able to estimate the anisotropy of radiative temperature as seen by a given sensor-sun-surface configuration.

Results from SUM to date have been constrained by the availability of observed surface temperatures for specific urban geometries. In this work, the canyon energy balance model of Mills (1997) is used to estimate surface temperatures for a range of simple urban geometries that are then modeled by SUM. This framework is used to assess the anisotropy for a range of urban geometries and different times of the year. This, and future work are intended to provide both a geography and climatology of urban thermal anisotropy and to provide a sensitivity analysis for the anisotropy as it is affected by factors that control the temperature of the urban surface. This approach provides an intermediate step towards a more fully coupled energy balance model with SUM that will be able to provide temperatures of urban surface facets for specific urban geometries

* Corresponding author address: James A. Voogt, Dept. of Geography, University of Western Ontario, London ON N6A 5C2 Canada; e-mail: javoogt@uwo.ca

2. METHODS

2.1 *Surface Characteristics*

Simulations are performed for two land use types: a light industrial area (LI) and a downtown area (DT). In each case, the urban surface is represented using a simple array of rectangular geometric shapes to represent the "buildings". For simplicity, the building footprints are square in these simulations. The surface geometric characteristics of the areas (building dimensions and street widths) are taken from Voogt and Oke (1997), and model simulations for the base case simulations (shown in red in Figure 2a,b) are set up so as to preserve the complete to plan area ratio (A_c/A_p) and roof to plan area ration (A_r/A_p) for those sites. For the surface geometry sensitivity studies, the dimensions are varied according to the height to width ratio (H/W) of the streets. For the seasonal sensitivity studies, the surface dimensions are fixed to correspond to those of the real study area.

2.2 *Modelled Surface Temperatures*

The surface temperatures are modeled using the urban canopy-layer climate model of Mills (1997). This model calculates the facet surface temperatures within a 3 x 3 array of buildings which themselves are surrounded by a solid wall for view factor and shading calculations (Mills 1997). The ground surface in this model is assumed to be completely asphalt covered. No latent heat flux is modelled. The resultant temperatures apply to the facet as a whole and are not subdivided into sunlit and shaded portions.

Table 1. Input surface parameters for the Mills (1997) urban canopy layer model. Values used are similar for both the LI and DT study areas.

Parameter	**roof**	**wall**	**ground**
surface	tar/gravel	brick	asphalt
albedo	0.15	0.2	0.2
emissivity	0.92	0.93	0.94
conductivity ($W\ m^{-1}\ K^{-1}$)	0.15	0.83	0.75
heat capacity ($J\ m^{-3}\ K^{-1} \times 10^6$)	1.0	1.37	1.94
density ($kg\ m^{-3}$)	0.05	1.83	2.11
thickness (m)	0.17	0.2	0.25

The boundary conditions for the model are specified from measured data collected at the LI site for the single day test that varies the building H/W, and from climatological normals based on data collected at Vancouver International Airport for the seasonal assessment. Input characteristics of the surface as required by the energy balance model are shown in Table 1 and sample output temperatures are shown in Figure 1.

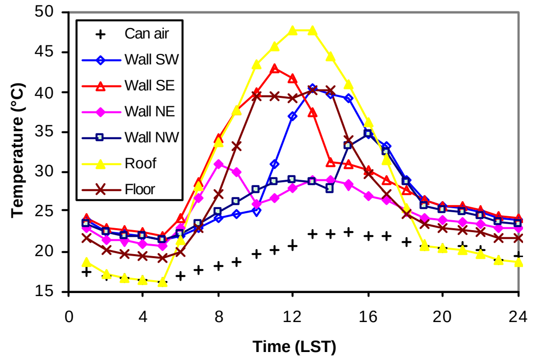

Figure 1. Modelled surface temperatures for the DT study area (Aug. 16, 1992) from the Mills (1997) model.

2.3 *Modelled Radiative Source Areas*

Radiative source areas are modeled using the SUM surface-sensor-sun relations model Soux et al. (2004). The SUM viewing parameters for the two sites are shown in Table 2. The larger plan area of the buildings in the LI area required that the surface array dimensions be set larger and the sensor position higher so as to reduce the sensitivity of the output to the absolute position of the projected FOV onto the building array.

Table 2. Input sensor characteristics for SUM.

Parameter	**Light Industrial**	**Downtown**
FOV	12°	
Sensor Height	750 m	450 m
View angles	5 – 45, 10° steps	
View azimuths	15 – 345, 15° steps	
Array dimensions	400 x 400 m	300 x 300 m

SUM can represent the urban surface using externally provided GIS information, or through an internal urban surface representation that can depict a variety of urban “block” layouts. Here, the urban surface is set to match that used with the urban canopy-layer model with the qualification that some adjustments of the absolute building dimensions are made in order to maintain the integer dimensions required by the SUM array and to preserve the H/W ratio of the streets specified in the energy balance model. The actual surface dimensions as used in SUM are shown in Table 3 with SUM using a 1 m x 1 m x 1 m grid resolution.

Radiative surface temperatures of the sunlit and shaded components of the urban surfaces must be provided to SUM from an independent source. Using this information SUM can generate estimates of the directional radiative temperature for a given sensor viewing position. Figure 2 illustrates the application of SUM to the case of a downtown area of Vancouver BC using observed facet surface temperatures.

Table 3 Surface dimensions (m) used in SUM and select non-dimensional surface parameters. Th input parameters H = building height, BL = building length and width, and SW = street width must be integer values in SUM. Bolded values are those used in the energy balance model, with the remaining values set by H/W.

Downtown (DT)					
H/W	H	BL & BW	SW	A_c/A_p	A_r/A_p
1	**15**	**18**	15	1.99	0.30
1.67	15	18	9	2.48	0.44
2	14	18	7	2.61	0.52
3	15	18	5	3.04	0.61
4	16	18	4	3.38	0.67
5	15	18	3	3.45	0.74
Light Industrial (LI)					
H/W	H	BL & BW	SW	A_c/A_p	A_r/A_p
0.25	**7**	**30**	28	1.25	0.27
0.6	6	25	10	1.49	0.51
1	7	30	7	1.61	0.66
2	8	30	4	1.83	0.78
3	9	30	3	1.99	0.83

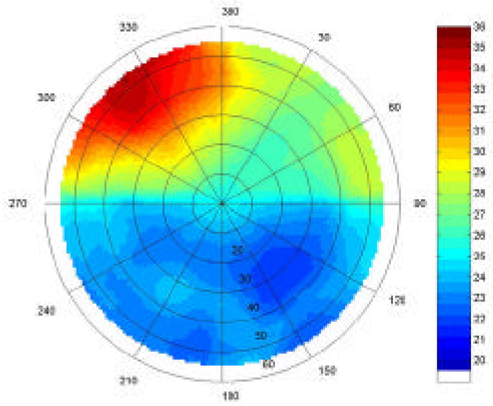

Figure 2. Polar plot of urban thermal anisotropy over the downtown area of Vancouver BC. August 16, 1992 for a 12° FOV airborne sensor (ht 525 m) solar Z=40°, AZ=145°. The colour scale is in °C. The primary street pattern of the area has azimuths of 45° and 135°.

Anisotropy here is represented by the maximum temperature difference or range from among all the viewing angles and azimuths tested. For the most part this yields maximum differences from large off-nadir view angles in opposing directions (typically in the up or down sun azimuth view directions). Other definitions are possible, e.g. the maximum difference between nadir and off-nadir observations and will be presented in future work.

3. RESULTS

3.1 *Variation with Surface Geometry*

Anisotropy is larger in the downtown area compared to the LI area (Figures 3a and 3b). In the results reported here, SUM simulations were only performed for the morning, ending at solar noon. Results may be expected to be similar, although not symmetric following solar noon because the temperature difference between facets is slightly larger in the morning due to the rapid increase in temperature of roof surfaces relative to road surfaces (see Figure 1).

Changes in anisotropy with decreasing zenith angle from sunrise onwards is not monotonic in all cases. In the LI area where the street pattern is aligned N/S and E/W the two most open geometries show a relative decrease between 08 and 10 LST. This is likely due to the relatively small roof-road temperature differences that occur here (most of the horizontal non-roof surface is not shaded) and the early peak in the difference between the east and west-facing wall temperatures.

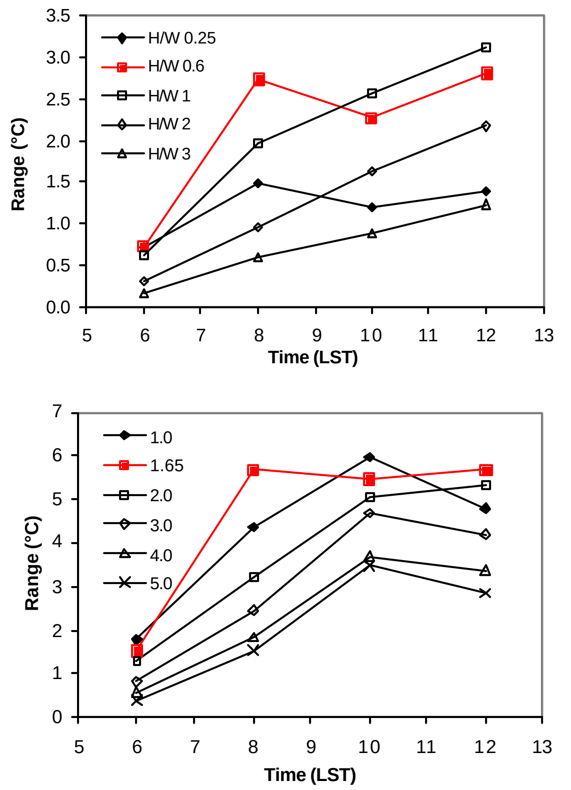

Figure 3. Modelled thermal anisotropy for a) Downtown and b) Light Industrial study areas with variable H/W ratios. Results for the "actual" H/W plotted in red.

Perhaps surprisingly, of the geometries tested, only H/W 1.0 exceeds the anisotropy modelled for the "actual" surface geometry. As the H/W increases, the absolute value of the anisotropy decreases substantially, forced due to the smaller wall temperature differences (more shading of wall surfaces) and in spite of a larger roof-horizontal temperature difference (more shading of canyon road surfaces).

In the DT area, anisotropy increases until approximately 10 LST followed by a decrease or reduced rate of increase until solar noon. This is related in part due to the relative azimuth angle with the street orientation (which is roughly 45°). The absolute magnitude of the anisotropy is again large for the low H/W ratios, and the actual surface geometry provides nearly the maximum at most of the modelled times. In the DT area, model results suggest significantly larger anisotropy compared to the LI study area, agreeing qualitatively with observed results. However the magnitude of the anisotropy tends to be somewhat lower than that observed. This underestimation is likely due in large part to the use of average facet temperatures rather than sunlit and shaded temperatures; neglect of vegetated surfaces and small scale shading of surfaces that is not incorporated in the models are also potential contributors. If air temperature is used to represent the shaded surface temperature components on the canyon walls and floor then the anisotropy is enhanced significantly, for example: H/W 1.0 for the LI area shows a nearly linear increase in anistropy with time with a peak value at LST of 5.8°C, over 2 degrees warmer than shown in Figure 3a.

3.2 *Seasonal Variations*

The seasonal variations of anisotropy for both study areas are summarized in Figure 4 using the base case surface geometries. Results are plotted for morning simulations only. Summertime anisotropy is largest and yields the largest differences between the two study areas for low solar zenith angles. Winter anisotropy is small.

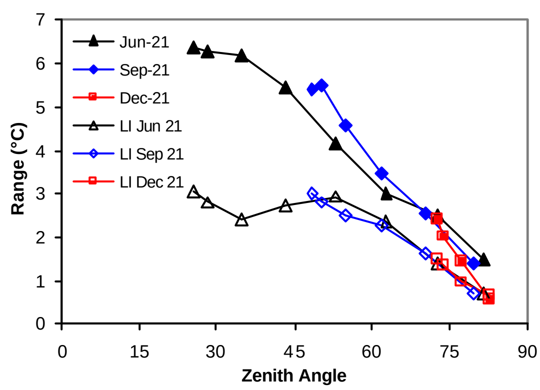

Figure 4. Variation of anisotropy (as represented by maximum temperature range) for the LI and DT study areas by season.

The anisotropy for Z < 50° is similar between seasons for each site with small differences between the sites and a similar slope of the anisotropy with zenith angle.

This infers that the temperature patterns are mostly controlled by Z and not particularly affected by the seasonal climatology. The only exception to this may be the results for the winter DT simulation at very large Z angles, possibly resulting from internal heating of the buildings. The similarity between seasons for similar Z may be an advantage in the search for simple empirical solutions to describe and correct for urban anisotropy, although confirmation of this awaits further sensitivity testing to specific meteorologic parameters such as wind speed. Above Z=50, different critical Z appear to characterize the two sites where the anisotropy shows much less variation with zenith angle, effectively resulting in a maximum effective anisotropy for that geometry.

Use of the Mills (1997) model alone also provides the ability to construct estimates of the overall urban surface temperature according to various definitions (e.g. see Voogt and Oke 1997) that may be useful in simple methods for correcting urban thermal anisotropy or as non-directionally biased estimates of urban surface temperature. Figure 5 illustrates the relation between the difference between plan and complete urban temperatures plan and air temperatures (canyon air temperatures estimated from the urban-canopy layer model). This comparison uses the most likely easily available estimate of urban remotely sensed temperature (a near-nadir estimate that may be used to represent the plan temperature) and a canopy-layer air temperature and combines them in a manner that may allow the complete temperature to be estimated. The complete temperature may be potentially useful for example when estimating the urban heat island using remote sensing.

The results shown in Figure 5 suggest that there is no simple seasonally independent estimate between the two differences plotted. Other combinations of variables also failed to show a simple nature to the relationship between plan and complete surface temperatures.

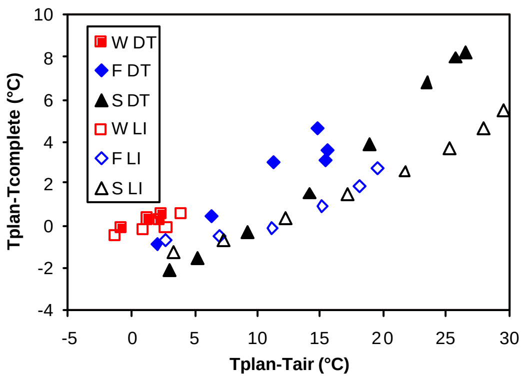

Figure 5. Composite plot of plan-complete surface temperature difference versus plan-air temperature for seasons (W=winter, F=fall, S=summer) and the two study areas (LI and DT).

4. CONCLUSIONS AND FUTURE WORK

This paper presents some initial results of modelled urban thermal anisotropy. The simulations use a non-coupled canopy layer energy balance model for the estimation of surface component temperatures and the SUM model for estimating the radiative source area of a remote sensor. The anisotropy is highly sensitive to surface geometry and solar zenith angle, to the extent that seasonal variations appear to be mostly dependent on solar zenith angle and not on the absolute meteorological conditions (clear skies are assumed). Further simulations to confirm the impact of meteorolgical parameters, such as wind, on the urban thermal anisotropy will be conducted. Simulations to assess the thermal anisotropy for cities located at different latitudes are also underway.

Somewhat surprising in these initial results is the suggestion that the actual surface geometries of two study areas provide nearly the largest anisotropy from among a range of H/W geometries tested. This finding may underscore the importance of anisotropy for large areal extents of urban surfaces, and not just those characterized by very tall buildings and large H/W. However, it should be kept in mind that the ground surface representation in both the canopy-layer model and the radiative source area model is highly simplified and does not represent the full range of surface structures known to be important to urban thermal anisotropy e.g. sloped roof surfaces, large trees and their shadows, and nor does it provide sunlit and shaded surface component temperatures directly that are shown here to be sensitive to the absolute magnitude of the modelled anisotropy. Further modelling and improvements to models are required to improve on these simulations.

Use of the canopy-layer energy balance model alone to assess relations between plan (nadir) and complete surface temperatures (a non-directionally biased estimate of the overall urban surface temperature) fail to identify any simple unique non-seasonal relationship that may easily be used to approximate the complete surface temperature.

5. REFERENCES

Lagouarde, J.P. et al. 2004. Airborne experimental measurements of the angular variations in surface temperature over urban areas : case study of Marseille (France). *Rem. Sens. Environ*. In press.

Mills, G. 1997: An urban canopy-layer climate model. *Theor. Appl. Climatol.*, **57**, 229-244.

Soux, A., Voogt, J.A. and T.R. Oke, 2004: A model to calculate what a remote sensor 'sees' of an urban surface. *Bound. Layer-Meteorol.*, **111**, 109-132.

Voogt, J.A. and T.R. Oke, 1998: Effects of urban surface geometry on remotely-sensed surface temperature. *Int. J. Rem. Sens*., **19**, 895-920.

Voogt, J.A. and T.R. Oke, 1997: Complete urban surface temperatures. *J. Appl. Meteor.*, **36**, 1117-1132.